A SCALING LAW FOR THE FLEXURAL MOTION OF FLOATING ICE

Colin Fox
Department of Mathematics, The University of Auckland
PB 92019 Auckland, New Zealand
fox@math.auckland.ac.nz

Abstract This paper presents a mathematical study of flexural motion of floating ice, including hydrodynamic effects, to derive a scaling law by reducing the deep-water dispersion equation to scale-independent form. The scaling shows that the well-known characteristic length, $l_c = \sqrt[4]{D/\rho g}$ and less well known characteristic time, $t_c = \sqrt{l_c/g}$, are unique in reducing solutions to canonical, scale-independent, form. The canonical solutions show that flexural motion is quasi-static for periods much greater than $2\pi t_c$, and is dynamic for shorter periods, with significant propagating waves. These conclusions are largely independent of the geometry of the ice sheet under consideration, the surrounding ice/water conditions, or distribution of applied forcing.

1. Introduction

The flexure of floating ice dominates its behaviour in the interaction between ocean waves and sea ice (Squire, 1978) and also in the interaction between slowly moving floating ice and sloping structures (Sodhi, 1987). The flexural response of typical sea ice occurs over length scales of roughly 20 metres to 2 kilometres and time scales of 2 seconds to 20 seconds, while the responses for lake ice and tank tests occur at shorter scales.

Fig. 1 shows a region of water of depth H which has some open water and some cover of uniform-thickness ice. We denote by Ω the region in the horizontal (x, y) plane that the ice covers. Over the time and length scales important for flexural motion, the ice is well modelled as a thin elastic plate with an effective flexural rigidity D, and the water can be taken to be an incompressible fluid with density ρ. I have shown the ice-water interface as a straight line, but that is not important for the conclusions here. Indeed, the scaling applies to any piece of floating ice

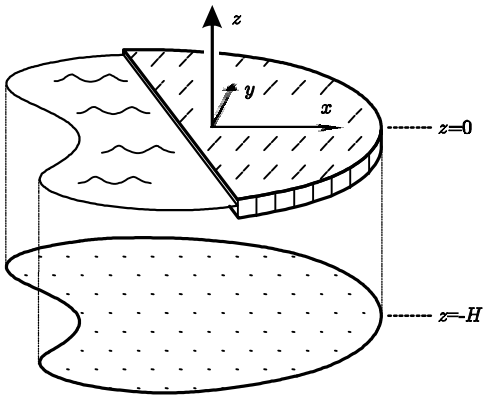

Figure 1. Schematic of a region of ice-covered water with the associated water column. The coordinate system is shown.

that has uniform flexural rigidity, independent of the shape of the ice sheet (or floe) and whether the surrounding water is open or has partial ice cover.

The scaling law derived here is relevant when we focus on the flexural motion of the ice cover. The main properties of the scaling are presented next, and in the remainder of the paper the scaling law is derived and the particular properties established in detail.

1.1. The scaling law in brief

In situations where the ice response is primarily flexural, it is most useful to scale length variables by the *characteristic length*, l_c, and time by the *characteristic time*, t_c, defined by

$$l_c = \left(\frac{D}{\rho g}\right)^{1/4} \qquad \text{and} \qquad t_c = \sqrt{\frac{l_c}{g}}, \tag{1}$$

respectively. The scaling has the following properties:

When the water is deep (I discuss what this means later), different situations that are geometrically equal in the non-dimensional variables $(\bar{x}, \bar{y}) = (x, y)/l_c$ have *almost exactly* the same flexural response as a function of $(\bar{x}, \bar{y})$ and the non-dimensional time $\bar{t} = t/t_c$. Hence, by using this scaling, tank tests can be designed to have flexural responses that are equivalent to field tests.

Scaling to non-dimensional variables has a second advantage which is that the canonical solutions, in the non-dimensional variables, allow us

to identify the distinct regimes of physical behaviour that occur in the flexure of floating ice. These regimes depend on the frequency (or rate) of the applied force, and are largely independent of the size or shape of the ice, or on the distribution of the applied force. At low forcing frequencies, specifically when $\bar{\omega} = \omega t_\mathrm{c} \ll 1$, the response is *quasi-static* with the ice motion being just the static flexural response moving in phase with the forcing. At high frequencies, $\bar{\omega} = \omega t_\mathrm{c} \gg 1$, the response is *dynamic* with travelling waves generated in the ice cover and the ice motion is not in phase with the forcing. At close to unit non-dimensional frequency, $\bar{\omega} = \omega t_\mathrm{c} \approx 1$, the force couples most effectively to the ice sheet and so the flexural response is generally dominated by this frequency. For example, an impact on the ice will generate a packet of waves with centre frequency close to $1/(2\pi t_\mathrm{c})$ and wavelength close to $2\pi l_\mathrm{c}$ that travels away from the impact with group and phase velocities nearly equal to $v_\mathrm{c} = l_\mathrm{c}/t_\mathrm{c}$.

This scaling is unique in reducing the response to canonical forms that depend on the scaled variables only. While other reductions to non-dimensional variables are sometimes used, they do not have the desirable property of simplifying considerations of ice flexure.

By examining the way the canonical solutions vary with water depth, we may also determine the water depth beyond which the ocean bottom does not affect the ice motion, i.e. the depth that can be considered 'deep'. When the force is applied locally, we find that the water is deep when $H/l_\mathrm{c} > 6$. When the force is applied coherently over an infinite line (not a situation that normally occurs in nature) the water needs to be approximately twice that depth to be deep, i.e. $H/l_\mathrm{c} > 12$. In particular, note that the depth that is deep depends only on the characteristic length – and hence the ice sheet flexural rigidity – and not on the wavelength of incoming waves as sometimes (mis)stated.

2. Derivation of the scaling law

In the remainder of this paper I substantiate these properties by deriving the scaling and establishing these properties in detail. The scaling is found by deriving a formal solution for the ice motion via a spectral expansion, writing the solution as an inverse transform involving the dispersion equation, then showing that any solution may be scaled to canonical form by scaling the dispersion equation.

2.1. Mathematical formulation

The vertical displacement of ice, $\eta\,(x, y, t)$, is related to the (upward) pressure applied on the ice, $p_\mathrm{a}\,(x, y, t)$ and the velocity potential in the

water $\phi(x,y,z,t)$, by the system of differential equations and boundary conditions (Greenhill, 1887; Fox and Squire 1994)

$$\begin{aligned} D\nabla^4_{x,y}\eta + m\eta_{tt} + \rho g\eta + \rho\phi_t &= p_{\mathrm{a}} \qquad z = 0 && \text{(2a)}\\ \eta_t &= \phi_z \qquad z = 0 && \text{(2b)}\\ \phi_z &= 0 \qquad z = -H && \text{(2c)}\\ \nabla^2_{x,y,z}\phi &= 0 \qquad -H < z < 0 && \text{(2d)} \end{aligned}$$

Eqn. 2a models a thin plate along with the linearized Bernoulli pressure. In the plate equation, the flexural rigidity, D, is often related to the ice-sheet effective Young's modulus, E, thickness, h, and Poisson's ratio, ν, via the expression $D = Eh^3/(12(1-\nu^2))$. The mass density m is related to the density of the ice, ρ_{i} by $m = h\rho_{\mathrm{i}}$. Eqn. 2b is the kinematic boundary condition between the water and ice, Eqn. 2c models a solid bottom, and Eqn. 2d represents the water being incompressible and inviscid.

2.2. Spectral solution

The dispersion equation arises from writing the forcing and ice motion as expansions over modes of the system. For physical systems like this one, where the physical properties are constant in time and piecewise constant in space, the modes are the wave-like functions $\mathrm{e}^{i(\omega t - \mathbf{k}\cdot(x,y))}$, where $\mathbf{k}$ is the vector wave-number in the (x,y)-plane and ω is the radial frequency. The restricted Fourier transform that gives the coefficients in a modal expansion of surface displacement is

$$\eta(\mathbf{k},\omega) = \int_T \int_\Omega \eta(x,y,t)\,\mathrm{e}^{\mathrm{i}(\mathbf{k}\cdot(x,y)-\omega t)} dxdydt \qquad (3)$$

and similarly for ϕ. We take the time interval $T = (-\infty,\infty)$ giving the usual Fourier transform to find the steady-state frequency response, or *transfer function*. Note that we use the same symbol for the transformed functions; the action of each function is implicitly determined by its arguments. We will calculate the inverse transform (over all wavenumber space $\mathbb{R}^2$) to give

$$\eta(x,y,\omega) = \int_{\mathbb{R}^2} \eta(\mathbf{k},\omega)\,\mathrm{e}^{\mathrm{i}(\omega t - \mathbf{k}\cdot(x,y))} d\mathbf{k} \qquad (4)$$

which is the spatially-dependent transfer function from forcing to displacement of the ice-covered region (and zero elsewhere). A similar inverse transform gives the potential $\phi(x,y,z,\omega)$.

Algebraic expressions for $\eta(\mathbf{k},\omega)$ and $\phi(\mathbf{k},z,\omega)$ can be found by transforming the differential equation 2a using the Green's identity

$$\begin{aligned}\int_\Omega \psi\nabla^4\eta\, d(x,y) &= \int_\Omega \eta\nabla^4\psi\, d(x,y) \\ &+ \int_{\partial\Omega}\left(\psi\nabla^3\eta - \nabla^2\eta\nabla\psi + \nabla\eta\nabla^2\psi - \eta\nabla^3\psi\right)\cdot dl\end{aligned}$$

and equation 2d using the Green's identity

$$\int_\Omega \psi\nabla^2\eta\, d(x,y) = \int_\Omega \eta\nabla^2\psi\, d(x,y) + \int_{\partial\Omega}\left(\psi\nabla\eta - \eta\nabla\psi\right)\cdot dl$$

and imposing the two boundary conditions 2b and 2c. Here dl is the outward surface element of the boundary $\partial\Omega$. Setting $\nabla = \nabla_{x,y}$, $\psi = \mathrm{e}^{i\mathbf{k}\cdot(x,y)}$, and writing $k = |\mathbf{k}|$, we find

$$\left(Dk^4 + \rho g - m\omega^2\right)\eta + \mathrm{i}\rho\omega\phi = p_\mathrm{a} + b_1 \tag{5a}$$

$$\phi_{zz} - k^2\phi = b_2 \tag{5b}$$

where the inhomogeneous terms $b_1(\mathbf{k},\omega)$ and $b_2(\mathbf{k},\omega)$ are given by the integrals over $\partial\Omega$. Since $\mathrm{e}^{i\mathbf{k}\cdot(x,y)}$ does not satisfy any particular boundary condition, these functions will depend on the solution which is unknown *a priori*. For our purposes we simply need to note that for physical problems, where displacements and velocities are finite, these terms are bounded linear functions of the forcing. The ordinary differential equation 5b may be solved along with the condition 2c to determine that the relation between ϕ and ϕ_z at the surface

$$k\tanh(kH)\,\phi(\mathbf{k},z,\omega)\,|_{z=0} + b_3(\mathbf{k},\omega) = \phi_z(\mathbf{k},z,\omega)\,|_{z=0}$$

where the function b_3 depends on the particular solution to 5b. Using the transformed version of Eqn. 2b then allows solution of Eqn. 5a to give the spectral solutions

$$\eta(\mathbf{k},\omega) = \frac{b(\mathbf{k},\omega)}{d(k,\omega)} \quad \text{and} \quad \phi(\mathbf{k},z,\omega) = \frac{b(\mathbf{k},\omega)}{d(k,\omega)}\frac{\mathrm{i}\omega\cosh k(z+H)}{\sinh kH} \tag{6}$$

where $b(\mathbf{k},\omega)$ is a linear function of the forcing that depends on the geometry, and $d(k,\omega)$ is the dispersion equation

$$d(k,\omega) = Dk^4 - m\omega^2 + \rho g - \frac{\rho\omega^2}{k\tanh kH}. \tag{7}$$

It suffices to consider the simplifying case where the geometry is such that $b(\mathbf{k},\omega)$ depends on $k = |\mathbf{k}|$ over its support; we will see two such

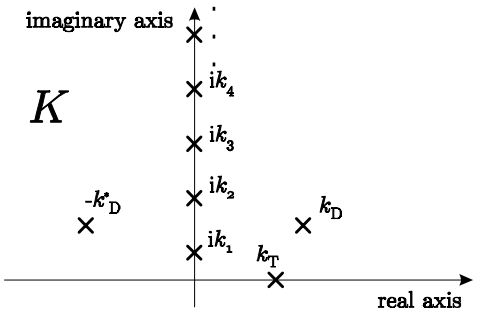

Figure 2. Schematic of the set K: roots of the dispersion equation in the upper half-plane.

cases in the next section. Then, for each ω, the integrals like 4 are over the real k-axis and can be performed as complex integrals by completing the contour in the upper complex k-plane. Hence the integral equals a sum over the poles of the integrand, which are the roots in the upper-half plane of $d(k,\omega)$. This set of roots of d is denoted K, and is shown (not to scale) in Fig. 2. The dispersion equation always has one positive real root k_{T} corresponding to a propagating wave, two complex roots with positive imaginary part, k_{D} and $-k_{\mathrm{D}}^{*}$, giving damped travelling waves, and a countably infinite number of pure positive imaginary roots, $\mathrm{i}k_n$ $n = 1, 2, \cdots$, each giving an evanescent wave (Fax and Squire, 1990).

Since d is even in k (as is b), we actually write $\eta(k,\omega)$ as the Mittag-Leffler expansion for each ω

$$\eta(k) = \frac{b(k)}{d(k)} = \sum_{q\in K} \frac{2qb(q)\,R(q)}{k^2 - q^2} \tag{8}$$

and similarly for ϕ. Here $R(q)$ is the residue of $1/d$ at the pole q,

$$R(q) = \left(\left.\frac{\partial d}{\partial k}\right|_{k=q} \right)^{-1}. \tag{9}$$

The details of the inverse transform depend on the way that b depends on k, and hence depends on the geometry, but is should be clear that for a given geometry the solution is entirely a function of the *position* of the roots of the dispersion equation.

2.3. Fundamental solutions

The simplest solutions are where unit harmonic force is applied at the origin of an infinite ice sheet, then $p_{\mathrm{a}} = \delta(x,y)\,\mathrm{e}^{\mathrm{i}\omega t}$, or along a line say

$y = 0$ when $p_\mathrm{a} = \delta(x)\,\mathrm{e}^{\mathrm{i}\omega t}$. Since there are no boundaries $b_1 = 0$ and $b_2 = 0$ in Eqns. 5, and so $b = 1$ in Eqns. 6 and 8, though the support is different for the two forcings. Substituting 8 into 4 and performing the simple integral (Abramowitz and Stegun, 1972 formula 11.4.44 with $\nu = 0$, $\mu = 0$, $z = -iq$ and $a = r$ and formula 9.6.4) gives the "free-space" fundamental solution, i.e. the response due to point forcing

$$\eta_\mathrm{P}(x,y) = \frac{i}{2}\sum_{q\in K} qR(q)\,H_0^{(1)}(qr) \tag{10}$$

where $H_0^{(1)}$ is a Hankel function of the first kind, and $r = \sqrt{x^2+y^2}$ is the distance from the point of forcing. The surface displacement for line forcing is given by a similar inverse transform resulting in the sum

$$\eta_\mathrm{L}(x,y) = i\sum_{q\in K} R(q)\exp(iq|x|). \tag{11}$$

2.4. Deep-water solutions

When the water is very deep, i.e. in the limit $H \to \infty$, the sum over the imaginary roots tends to an integral over the positive imaginary semi-axis. After considerable calculation it is possible to write the resulting solutions as sums over the roots of the *modified* deep-water dispersion equation (Eqn. 7 with $H \to \infty$) for $\mathrm{Re}(k) > 0$, analytically continued to the whole complex k-plane:

$$Dk^5 + \left(\rho g - m\omega^2\right)k - \rho\omega^2 = 0. \tag{12}$$

Let $K_\mathrm{d} = \{k_\mathrm{T}, k_\mathrm{D}, k_\mathrm{D}^*, k_\mathrm{E}, k_\mathrm{E}^*\}$ denote the set of roots (k_T and k_D as before, k_E has positive imaginary and negative real parts). The residue of η at a pole $q \in K_\mathrm{d}$ is

$$R_\mathrm{d}(q) = \frac{q^2}{5\rho\omega^2 - 4\left(\rho g - m\omega^2\right)q}. \tag{13}$$

Note that the residues at k_T, k_D and k_D^*, are the same as defined previously in Eqn. 9, and we denote these R_T, R_D and R_D^*, respectively. Write $R_\mathrm{E} = R_\mathrm{d}(k_\mathrm{E})$ and hence $R_\mathrm{E}^* = R_\mathrm{d}(k_\mathrm{E}^*)$. The response to point forcing in the deep-water limit can be written in terms of these poles of η as

$$\begin{aligned}\eta_\mathrm{P}(r) = {} & \frac{i}{2}k_\mathrm{T}R_\mathrm{T}H_0^{(1)}(k_\mathrm{T}r) - \frac{k_\mathrm{T}R_\mathrm{T}}{4}h(k_\mathrm{T}r) - \mathrm{Im}\left[k_\mathrm{D}R_\mathrm{D}H_0^{(1)}(k_\mathrm{D}r)\right] \\ & - \frac{1}{2}\mathrm{Re}\left(k_\mathrm{D}R_\mathrm{D}h(k_\mathrm{D}r)\right) + \frac{1}{2}\mathrm{Re}\left(k_\mathrm{E}R_\mathrm{E}h(-k_\mathrm{E}r)\right),\end{aligned} \tag{14}$$

where $h(qr) = \mathbf{H}_0(qr) - Y_0(qr)$. The response to line forcing in the deep water limit can be written as,

$$\eta_{\mathrm{L}}(r) = iR_{\mathrm{T}} \exp(ik_{\mathrm{T}} r) + \frac{R_{\mathrm{T}}}{\pi} g(k_{\mathrm{T}} r) - 2\,\mathrm{Im}\left[R_{\mathrm{D}} \exp(ik_{\mathrm{D}} r)\right] + \frac{2}{\pi}\,\mathrm{Re}\left[R_{\mathrm{D}} g(k_{\mathrm{D}} r)\right] + \frac{2}{\pi}\,\mathrm{Re}\left[R_{\mathrm{E}} g(-k_{\mathrm{E}} r)\right] \quad (15)$$

where $g(qr) = -\mathrm{Ci}(qr)\cos(qr) - \mathrm{si}(qr)\sin(qr)$. The terms in equations 14 and 15 involving the functions h and g are the contributions from the integrals over the imaginary axis.

Graphs of these solutions are given in section 5.

3. Scaling

The scaling to normalized (and non-dimensional) form is based on the structure of the roots of the modified deep-water dispersion Eqn.12. Since deflections given in Eqns. 14 and 15, are continuous functions of the roots, simplifying the structure of the roots corresponds to simplification of the solutions.

When k is small, ω is also small, giving $k^5 \approx 0$, $\left|m\omega^2\right| \ll \rho g$, and hence $k \approx \omega^2/g$. Thus for long wavelengths, and hence long periods, the dispersion equation is the same as for water waves with $k \propto \omega^2$ and with no dependence on the ice-sheet thickness or mass density m.

On the other hand when k is large, ω is also large, and for typical values of m we find that $Dk^5 \gg \left|\left(\rho g - m\omega^2\right) k\right|$ and hence $k \approx \left(\rho\omega^2/D\right)^{1/5}$. Thus for short wavelengths, and short periods, $k \propto \omega^{2/5} h^{-3/5}$. The dependence of k on ice sheet thickness h comes via the flexural rigidity, but note that again the effective dispersion equation is not dependent on the ice-sheet mass density.

The two relations $k \approx \omega^2/g$ and $k \approx \left(\rho\omega^2/D\right)^{1/5}$ are straight lines on a $\log k$ - $\log \omega$ graph which intersect at the point $k = \sqrt[4]{\rho g/D}$ and $\omega = \sqrt[8]{\rho g^5/D}$ (for example see Fox and Squire (1994) figure 2). The $\log k$ - $\log \omega$ graphs for different values of D can be made to coincide by putting the intersection at the common point (1,1) via the scaling to normalized variables $\bar{k} = k l_{\mathrm{c}}$ and $\bar{\omega} = \omega t_{\mathrm{c}}$ by the characteristic length and time defined in equation 1.

The resulting graph of scaled roots of the dispersion equation as a function of $\bar{\omega}$ is shown in Fig. 3 for three values of flexural rigidity, D, corresponding to ice-sheet thicknesses of $h = 0.1$ m, $h = 1$ m, and $h = 10$ m when the effective Young's modulus takes the typical value of 5×10^9 Pa and the density of ice is $\rho_{\mathrm{i}} = 922.5$ kg m^{-3}. The magnitude of the real and imaginary parts of the three roots $\bar{k}_{\mathrm{T}}$, $\bar{k}_{\mathrm{D}}$, and $\bar{k}_{\mathrm{E}}$, are

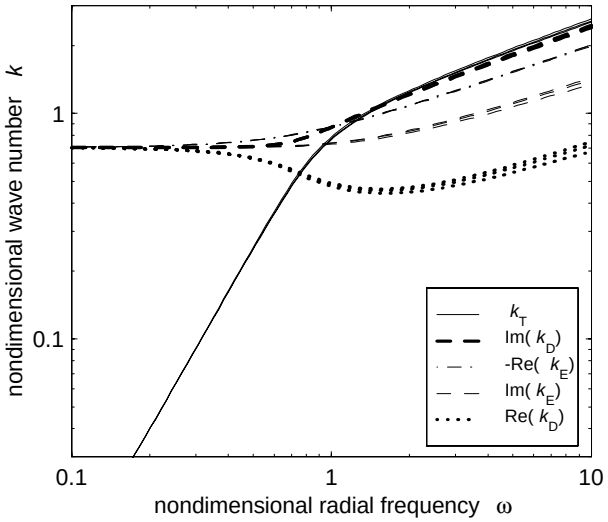

Figure 3. Graph of k_{T} (log scale) and the real and imaginary parts of k_{D} and k_{E} as a function of $\bar{\omega}$ (log scale) for three flexural rigidities corresponding to ice thicknesses h of 0.1, 1 and 10 metres.

graphed. Increasing h corresponds to increasing $\bar{k}_{\mathrm{T}}$ and $\mathrm{Im}\left(\bar{k}_{\mathrm{D}}\right)$ (the upper two sets of curves for $\bar{\omega} > 2$) and to decreasing values of $-\mathrm{Re}\left(\bar{k}_{\mathrm{D}}\right)$, $\mathrm{Im}\left(\bar{k}_{\mathrm{E}}\right)$ and $\mathrm{Re}\left(\bar{k}_{\mathrm{E}}\right)$ (the lower three sets of curves for $\bar{\omega} > 2$).

Note that the scaling has the effect of making the three scaled curves for the travelling-wave number, $\bar{k}_{\mathrm{T}}$, very nearly identical for all frequencies, and the curves of the real and imaginary parts of the other roots near to overlapping. Hence, this scaling to non-dimensional variables reduces the solutions to a canonical solution depending on $\bar{\omega}$ only – and is unique in achieving that.

It is interesting to note that other non-dimensional formulations are possible which do not give a useful reduction to canonical solutions for the range of parameters typical in sea ice dynamics. For example, at very large k, $\left|\left(\rho g - m\omega^2\right)\right| k \gg \rho\omega^2$ and $m\omega^2 \gg \rho g$ giving the asymptote $k \approx \left(m\omega^2/D\right)^{1/4}$. Putting the intersection of this relationship and the small-k relationship at a common point leads to a different characteristic length and time than derived above. This scaling would be relevant in cases where ice has ten times its actual density (though then the ice sheet would sink). However, it does not have the property of making the wave-number vs frequency graphs overlap for typical mass densities and for periods where the solutions are appreciable.

4. Quasi-static and dynamic regimes

Fig. 3 also shows that the non-dimensional frequency $\bar{\omega} = 1$ sets a transition between distinct regimes in the frequency-wavelength relationship, and hence in the mechanism that dominates the ice flexure. The identification of the distinct regimes of behaviour is the most valuable consequence of the scaling law.

At low frequencies, $\bar{\omega} \ll 1$, we see $\bar{k}_{\mathrm{T}} \approx 0$ while $\bar{k}_{\mathrm{D}} \simeq (1+\mathrm{i})/\sqrt{2}$ and $\bar{k}_{\mathrm{E}} \simeq (-1+\mathrm{i})/\sqrt{2}$. Since $R_{\mathrm{T}} \to 0$ as $\bar{k}_{\mathrm{T}} \to 0$, the coefficient of any travelling wave is small and the solution is reduced to the contributions due to the complex roots, only. Thus the range $\bar{\omega} \ll 1$ has just the single *quasi-static* solution which is essentially the static solution moving in phase with the harmonic loading. In this regime inertial effects are negligible.

At high frequencies, $\bar{\omega} \gg 1$, $\bar{k}_{\mathrm{T}}$ is no longer small and the solution is *dynamic* since an appreciable travelling wave is generated by the forcing. In this regime $\bar{k}_{\mathrm{T}} \approx \bar{\omega}^{2/5}$, and hydrodynamic effects play a significant role in the ice flexure.

The region $\bar{\omega} \approx 1$ sets a range of intermediate behaviour in which the coupling between the load and the ice sheet is greatest. This frequency will dominate the flexural response when the forcing contains a range of frequencies.

4.1. The approximation $m = 0$

Fig. 3 shows that the locus of the three roots made nearly identical, for a wide range of ice thicknesses, by using a scaling based on the flexural rigidity only; the effect of thickness via mass density is not significant. Hence setting $m = 0$ does not greatly affect the solutions. However, the small difference in the positions of the roots, for differing m for given D, does cause a difference in solutions which is primarily a decrease in the wavelength of the travelling wave with increasing m. The same decrease in wavelength occurs, to first order, by setting $m = 0$ and increasing frequency by the multiplicative factor $(1 + mk_{\mathrm{T}}/2)$.

5. Canonical solutions

Fig. 4 shows the response to point forcing as a function of non-dimensional distance from the forcing, r, in the low frequency ($\bar{\omega} = 0.2$), unit frequency, and high frequency ($\bar{\omega} = 5.0$) regimes. The real and imaginary parts of the solution are shown for infinite water depth, calculated using Eqn. 14. The solutions for the finite depth $H/l_{\mathrm{c}} = 2\pi$, calculated using Eqn. 10 are visually identical to the graphs shown. Note that at low

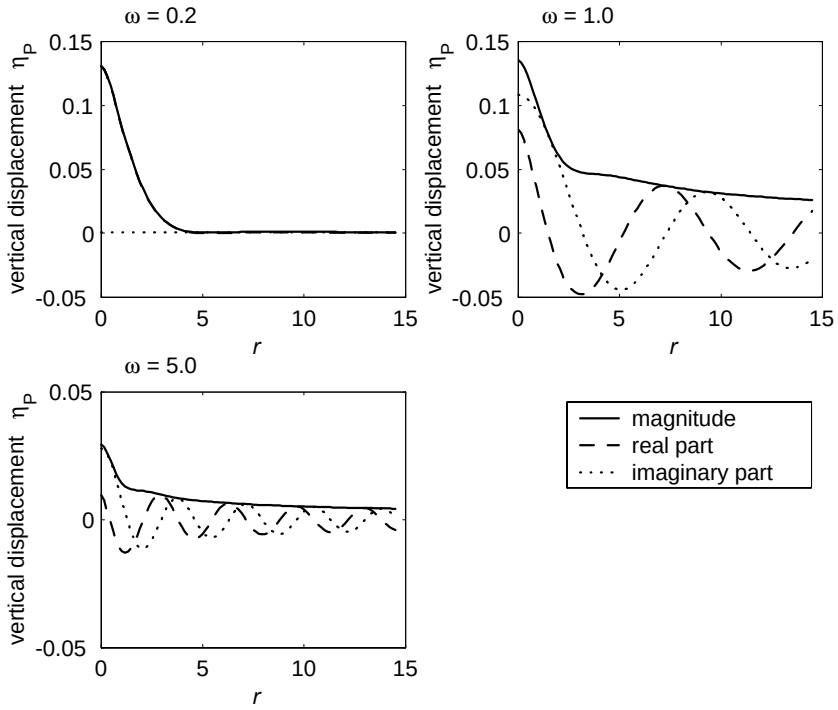

Figure 4. Magnitude, real part and imaginary part of displacement for point forcing at non-dimensional frequencies 0.2, 1.0, and 5.0, as a function of non-dimensional distance from the point of forcing, assuming deep water.

frequencies only the real part of the solution is appreciable and hence the response is in phase with the forcing. For frequencies above about unit nondimensional frequency the imaginary part of the solution is appreciable, actually larger than the real part near the point of forcing, and so energy is transferred into the ice, with amplitude of the travelling wave being greater for $\bar{\omega} = 1$ than $\bar{\omega} = 5$.

Canonical solutions for line forcing are shown in Fig. 5, also as a function of non-dimensional distance from the line of forcing, $|x|$, in the three frequency regimes. For line forcing, the solutions in the low frequency regime differ for infinite water depth and for $\bar{H} = 2\pi$, and so the solution for $\bar{H} = 2\pi$ and $\bar{\omega} = 0.2$ has been included. At the higher frequencies $\bar{\omega} = 1.0$ and $\bar{\omega} = 5.0$ the solutions for the two depths are visually identical.

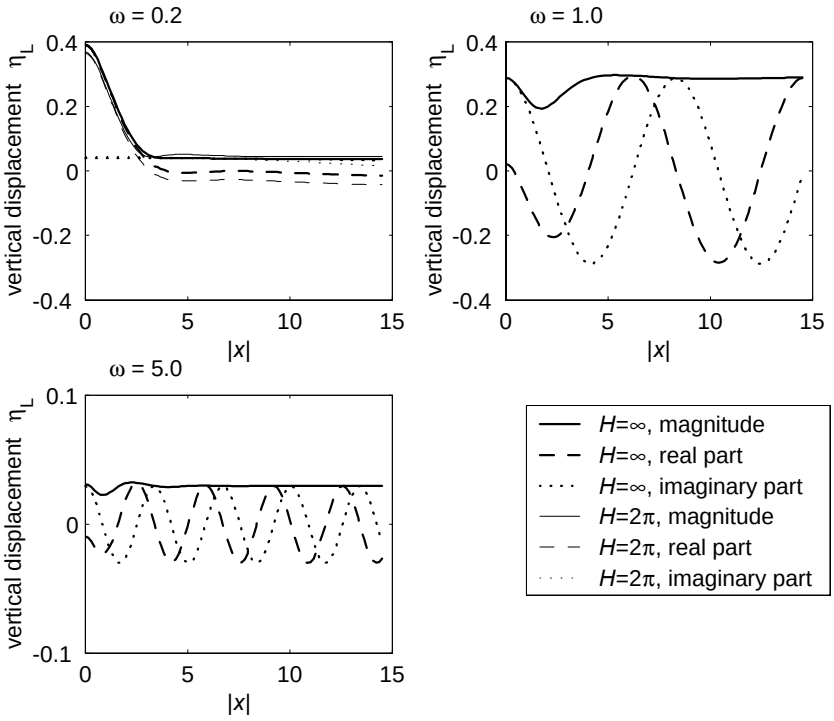

Figure 5. Magnitude, real part and imaginary part of displacement as a function of non-dimensional distance from line forcing at non-dimensional frequencies 0.2, 1.0, and 5.0. For $\bar{\omega} = 0.2$ the depths $\bar{H} = 2\pi$ and $\bar{H} = \infty$ are shown, while for the other frequencies only the response for $H = \infty$ is shown.

5.1. Water depth

Figs. 6 and 7 show the real (in-phase with the forcing) and imaginary (in quadrature to the forcing) parts of the solutions at the location of forcing for three scaled water depths, $\bar{H} = H/l_c$, as a function of normalized frequency.

We can conclude from these figures that the depth beyond which the water may be considered to be effectively infinitely deep depends on the nature of the forcing. For forcing that is localized and may be treated as a point, non-dimensional water depths greater than 2π, i.e. actual depths approximately 6 times the characteristic length, are deep for any rate of forcing. However, for forcing that occurs along a line, the non-dimensional depth 2π is not deep, particularly for low-frequency forcing. Instead, actual depths of 12 times the characteristic length are required for the water to be deep at any rate of forcing.

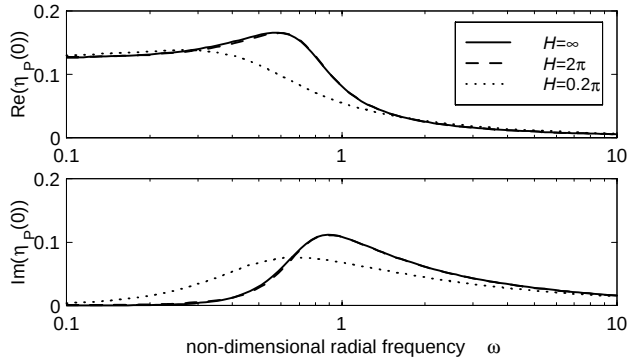

Figure 6. Real and imaginary parts of the displacement at the point of forcing as a function of normalized frequency, for three non-dimensional water depths.

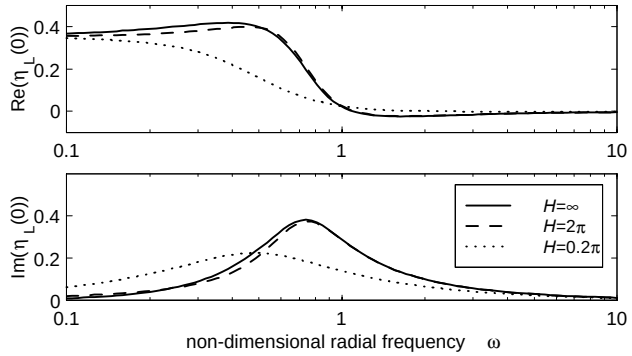

Figure 7. Real and imaginary parts of the displacement at the line of forcing as a function of normalized frequency, for three non-dimensional water depths.

5.2. Velocity effects

The characteristic velocity $v_c = l_c/t_c$ sets the boundary between regimes of behaviour in the response to moving loads of ice floating on moderately deep water (Squire and others, 1996). Since the travelling wave with unit normalized frequency has period $2\pi t_c$ and wavelength $2\pi l_c$, v_c is the phase speed of the dominant propagating wave. Note that the slope of the $\log k$ versus $\log \omega$ graph equals the ratio of group speed to phase speed. These two speeds are equal when the slope in Fig. 3 equals 1 which also occurs at unit normalized frequency.

6. Conclusions

It has been shown that the characteristic length, derived by Wyman (1950) for the static case, gives the appropriate length scale for *both* static and dynamic responses. The characteristic time gives the natural scaling in time that separates the response into quasi-static and dynamic regimes. Since the scaling reduces the dispersion relation to a single graph, any dependence of the scaling on physical parameters was effectively removed and therefore we may conclude that the scaling applies to any geometry or applied forcing.

Scaling by characteristic length and time is therefore the best way of comparing field tests and laboratory tests of ice flexure. Consequently, measurement of characteristic length (or time) gives the primary property of a floating ice sheet that determines its flexural response. In contrast, the ice thickness h, for a given flexural rigidity D, plays a very minor role in determining the flexural dynamics.

Once the characteristic length of a floating ice sheet is known, even approximately, the water is known to be deep if $H > 6l_c$ for point forcing, or $H > 12l_c$ for line forcing.

Acknowledgments

The author is grateful to John Dempsey and Vernon Squire for helpful discussions, and to the Marsden Fund for financial support.

References

Abramowitz, M. & Stegun, I.A. 1972. *A Handbook of Mathematical Functions*. Dover Publications, New York.

Fox, C., and V.A. Squire. 1990. Reflexion and transmission characteristics at the edge of shore fast sea ice. *J. geophys. Res.* **95**, 11629-11639.

Fox, C., and Squire, V.A. 1994. On the Oblique Reflexion and Transmission of Ocean Waves at Shore Fast Sea Ice. *Phil. Trans. R. Soc. Lond.* A **347**, 185-218.

Greenhill, A. G. 1887. Wave motion in hydrodynamics, *Am. J. Math.*, **9**, 62-112.

Squire, V. A., R. J. Hosking, A. D. Kerr and P. J. Langhorne. 1996. *Moving loads on ice plates*. Dordrecht, The Netherlands, Kluwer Academic Press.

Sodhi, D. S., 1987. *Dynamic analysis of failure modes of ice sheets encountering sloping structures*, ASME Proc. 5th Int. Offshore Mech. Arctic Eng. Conf., Houston, Texas (ed. V. J. Lunardini, N. K. Sinha, Y. S. Wang & R. D. Goff), vol. IV, 121-124.

Squire, V. A. 1978. *Dynamics of ocean waves in a continuous sea ice cover*. Ph.D. dissertation, 191 pp., Univ. of Cambridge, England.

Wyman, M. 1950. Deflection of an infinite plate, *Canadian Journal of Research*, **28** A 293-302.